

We are IntechOpen, the world's leading publisher of Open Access books Built by scientists, for scientists

5,000

Open access books available

125,000

International authors and editors

140M

Downloads

Our authors are among the

154

Countries delivered to

TOP 1%

most cited scientists

12.2%

Contributors from top 500 universities



WEB OF SCIENCE™

Selection of our books indexed in the Book Citation Index
in Web of Science™ Core Collection (BKCI)

Interested in publishing with us?
Contact book.department@intechopen.com

Numbers displayed above are based on latest data collected.
For more information visit www.intechopen.com



Diffusion Theory for Cell Membrane Fluorescence Microscopy

Minchul Kang

Abstract

Since the discovery of fluorescent proteins and the development of DNA recombinant techniques, various fluorescence methods have significantly improved our understanding of cell biology at a molecular level. In particular, thanks, in large part, to technological advances in these fields, fluorescence techniques such as fluorescence recovery after photobleaching (FRAP), fluorescence correlation spectroscopy (FCS), and single-particle tracking (SPT) have become standard tools in studying cell membrane structure as well as the diffusion and interaction of biomolecules in the cell membrane. In this chapter, we will review some topics of the diffusion theory from both deterministic and probabilistic approaches, which are relevant to cell membrane fluorescence microscopy. Additionally, we will derive some basic equations for FRAP and FCS based on the diffusion theory.

Keywords: diffusion theory, fluorescence recovery after photobleaching, fluorescence correlation spectroscopy, cell membranes

1. Introduction

Diffusion is an idealization of the random motion of one or more particles in space. Since diffusion is a dominant way for biological organisms to transport various molecules to desirable locations for cell signaling, the role of diffusion within biological systems is critical [1–3]. Therefore, to quantify the diffusion coefficient, a measure of diffusion rates, is essential to understand both the physiology and pathology of cells in terms of cell signaling time scales [1–3]. Moreover, the diffusion coefficients of proteins may also provide information on the landscape of the membrane environment where diffusion occurs [4–6]. However, quantifying the diffusion especially in live cell membranes is still challenging although a couple of tools are available including fluorescence recovery after photobleaching (FRAP) and fluorescence correlation spectroscopy (FCS) [7, 8]. Diffusion is quantified by a diffusion coefficient, D , which characterizes the proportionality in a linear relationship between mean squared displacement (MSD, $\langle x^2 \rangle$) of a Brownian particle and time [9, 10]. To determine the diffusion coefficients of biomolecules of interests, mathematical models for the diffusion process are compared with experimental data in FRAP and FCS analysis. In this chapter, we bridge the gap between experimental and theoretical aspects of FRAP and FCS by reviewing mathematical theories for FRAP and FCS.

2. Diffusion equation

2.1 Diffusion equation from the deterministic point of view

In 1855, Fick [11] published two cornerstone papers on diffusion, in which he proposed the fundamental laws describing the transport of mass due to the concentration gradient and an associated mathematical model. According to Fick's first law, the diffusive flux (J) is proportional to the concentration gradient of diffusants (du/dx) with a proportionality constant called a diffusion coefficient, D . In one-dimensional spatial dimension (\mathbb{R}^1), Fick's law can be represented as

$$J = -D \frac{du}{dx} \quad (1)$$

where $J(x, t)$ is the diffusion flux and $u(x, t)$ is the concentration of diffusants at the location x at time t . The diffusion coefficient can be calculated by the Stokes-Einstein equation [12, 13]:

$$D = \frac{k_B T}{6\pi\eta r} \quad (2)$$

where k_B is Boltzmann's constant, T is the absolute temperature, η is the dynamic viscosity, and r is the radius of the spherical particle. Assuming the conservation of mass in an infinitesimal interval $(x, x + \Delta x)$, we obtain

$$\begin{aligned} \frac{\partial}{\partial t} \{u(x, t)\Delta x\} &= J(x, t) - J(x + \Delta x, t); \\ \frac{\partial u}{\partial t} &= \frac{J(x, t) - J(x + \Delta x, t)}{\Delta x} \end{aligned} \quad (3)$$

where $u(x, t)\Delta x$ is the total number of molecules in the interval $(x, x + \Delta x)$ and $J(x, t) - J(x + \Delta x, t)$ is the difference of influx and efflux in and out of the interval (i.e., net change in the total number of molecules in the interval) as shown in **Figure 1**.

By combining Eqs. (1) and (3) and by taking the limit in $\Delta x \rightarrow 0$, we have Fick's second law that describes the diffusion process in a form of partial differential equation:

$$\frac{\partial u}{\partial t} = D \frac{\partial^2 u}{\partial x^2} \quad (4)$$

Eq. (4) is often referred to as the one-dimensional diffusion equation or heat equation. Similarly, two-dimensional (\mathbb{R}^2) and three-dimensional (\mathbb{R}^3) can be derived as

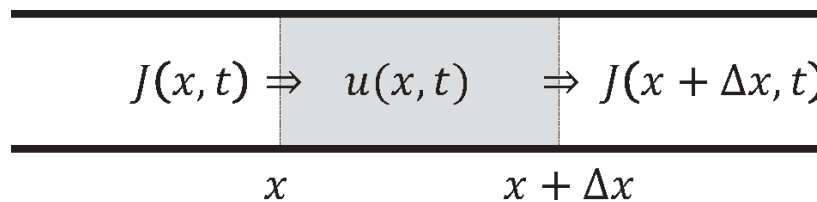


Figure 1.
The change in the number of molecules in an intestinal interval due to diffusion.

$$\begin{aligned}\frac{\partial u}{\partial t} &= D \left(\frac{\partial^2 u}{\partial x^2} + \frac{\partial^2 u}{\partial y^2} \right) \\ \frac{\partial u}{\partial t} &= D \left(\frac{\partial^2 u}{\partial x^2} + \frac{\partial^2 u}{\partial y^2} + \frac{\partial^2 u}{\partial z^2} \right)\end{aligned}\quad (5)$$

In a more compact form, the diffusion equations are written using the Laplace operator, Δ :

$$u_t = D\Delta u \quad (6)$$

where $\Delta u = \frac{\partial^2 u}{\partial x^2}$ in \mathbb{R}^1 , $\Delta u = \frac{\partial^2 u}{\partial x^2} + \frac{\partial^2 u}{\partial y^2}$ in \mathbb{R}^2 , and $\Delta u = \frac{\partial^2 u}{\partial x^2} + \frac{\partial^2 u}{\partial y^2} + \frac{\partial^2 u}{\partial z^2}$ in \mathbb{R}^3 .

Importantly, the diffusion equation satisfies the following important properties:

1. **Property 1: Translation invariance.** If $u(x, t)$ is a solution of the heat equation, then for any fixed number x_0 , the function $u(x - x_0, t)$ is also a solution.
2. **Property 2: Derivatives of solutions.** If $u(x, t)$ is a solution of the heat equation, then the partial derivatives of u also satisfy the heat equation.
3. **Property 3: Integrals and convolutions.** If $\Phi(x, t)$ is a solution of the heat equation, then $\Phi * g$ (the convolution of Φ with g) is also a solution where $\Phi * g(x, t) = \int_{-\infty}^{\infty} \Phi(x - y, t)g(y)dy$ provided that this improper integral converges. The improper integral $\Phi * g$ is called the convolution of Φ and g .
4. **Property 4: Dilation.** Suppose $a > 0$ is a constant. If $u(x, t)$ is a solution of the heat equation, then the dilated function $v(x, t) = u(\sqrt{a}x, at)$ is also a solution.

Based on these properties, we are now ready to solve the following initial value problem on $x \in \mathbb{R}^1$ for $0 \leq t < \infty$:

$$\begin{cases} u_t = Du_{xx} \\ u(x, 0) = H(x) \end{cases} \quad \text{where } H(x) = \begin{cases} 1, & x > 0 \\ 0, & x \leq 0 \end{cases} \quad (7)$$

where $H(x)$ is often referred to as the Heaviside function.

By **Property 4**, any solution $(u(x, t))$ is unaffected by the dilation $x \mapsto \sqrt{a}x$ and $t \mapsto at$ for any $a \in \mathbb{R}^1$. Since $\frac{x}{\sqrt{t}}$ is also unaffected by the dilations $(\frac{x}{\sqrt{t}} \mapsto \frac{\sqrt{a}x}{\sqrt{at}} = \frac{x}{\sqrt{t}})$, we look for a solution in the form of $g\left(\alpha \frac{x}{\sqrt{t}}\right)$ for some constant α . Notice also that $g\left(\alpha \frac{x}{\sqrt{t}}\right)$ is also invariant under these dilations: $g\left(\alpha \frac{\sqrt{a}x}{\sqrt{at}}\right) = g\left(\alpha \frac{x}{\sqrt{t}}\right)$. If we let $p = \alpha \frac{x}{\sqrt{t}}$ and choose $\alpha = \frac{1}{\sqrt{4D}}$, then by the chain rule, we have

$$0 = u_t - Du_{xx} = -\frac{p}{2t}g'(p) - \frac{\kappa}{4Dt}g''(p) = -\frac{1}{4t}\{g''(p) + 2pg'(p)\} \quad (8)$$

which reduces to an ordinary differential equation $g'' + 2pg' = 0$. This can be solved as.

$$g = C_2 + \int_0^p C_1 e^{-r^2} dr \quad \text{where } g(0) = C_2 \quad (9)$$

for arbitrary constants C_1 and C_2 . Because as $t \rightarrow 0+$, $p \rightarrow \infty$, for $x > 0$

$$1 = \lim_{t \rightarrow 0+} u(x, t) = C_2 + \int_0^{\infty} C_1 e^{-r^2} dr = \frac{\sqrt{\pi}}{2} C_1 + C_2 \quad (10)$$

where we used a well-known identity (the error function integral):

$$\int_{-\infty}^{\infty} e^{-ax^2} dx = \sqrt{\frac{\pi}{a}}, \quad (11)$$

On the other hand, since as $t \rightarrow 0+$, $p \rightarrow -\infty$, for $x < 0$

$$0 = \lim_{t \rightarrow 0+} u(x, t) = C_2 + \int_0^{-\infty} C_1 e^{-r^2} dr = -\frac{\sqrt{\pi}}{2} C_1 + C_2 \quad (12)$$

which implies that $C_1 = \frac{1}{\sqrt{\pi}}$ and $C_2 = \frac{1}{2}$. Putting together, we have a solution

$$u(x, t) = \frac{1}{2} + \frac{1}{\sqrt{\pi}} \int_0^{x/\sqrt{4kt}} e^{-r^2} dr \quad (13)$$

Define $\Phi(x, t) = u_x(x, t)$; then

$$\begin{aligned} \Phi(x, t) &= \frac{\partial}{\partial x} \left(\frac{1}{2} + \frac{1}{\sqrt{\pi}} \int_0^{x/\sqrt{4kt}} e^{-r^2} dr \right) \\ &= \frac{1}{\sqrt{\pi}} e^{-\frac{x^2}{4kt}} \cdot \frac{1}{\sqrt{4kt}} \\ &= \frac{1}{\sqrt{4\pi kt}} e^{-\frac{x^2}{4kt}} \end{aligned} \quad (14)$$

By **Property 2, derivatives of solutions**, the function $\Phi(x, t) = \frac{1}{\sqrt{4\pi kt}} e^{-\frac{x^2}{4kt}}$ is also a solution to the diffusion equation. $\Phi(x, t)$ is called the (one-dimensional) heat kernel or the fundamental solution of the heat equation. The graphs of the heat kernel for different t are shown in **Figure 2**.

From **Figure 2**, we can see that the heat kernel $\Phi(x, t)$ has a “bell curve” graph of a normal distribution (Gaussian function) with $\sqrt{2Dt}$ as the standard deviation, which sometimes called the Gaussian root mean square width. Also, $\frac{1}{\sqrt{4\pi t}}$ modulates the amplitude of the Gaussian curves, and the amplitude blows up to ∞ as $t \rightarrow 0+$ and approaches 0 as $t \rightarrow \infty$, i.e.:

$$\lim_{t \rightarrow 0+} \Phi(x, t) = \begin{cases} 0 & \text{if } x \neq 0 \\ \infty & \text{if } x = 0 \end{cases}. \quad (15)$$

Also, from the error function integration (Eq. (14))

$$\begin{cases} \int_{-\infty}^{\infty} \Phi(x, t) dx = 1, \text{ for all } t \geq 0 \\ \int_{-\infty}^{\infty} \Phi(x - y, t) dx = 1, \text{ for all } t \geq 0 \end{cases} \quad (16)$$

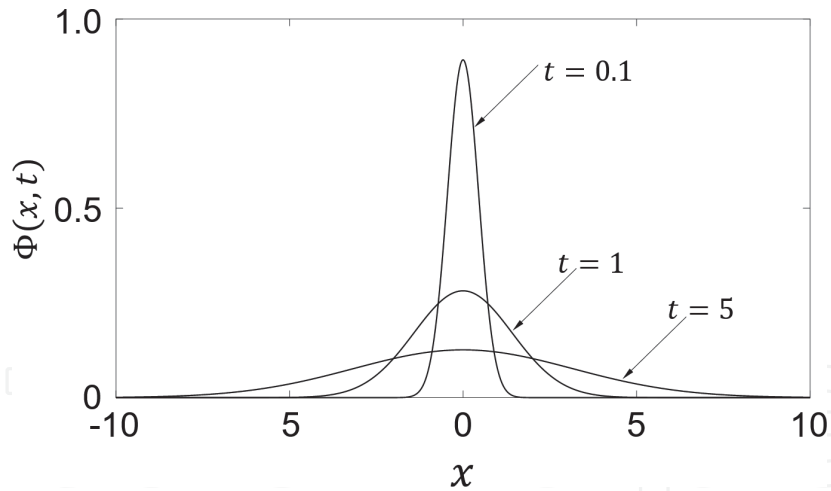


Figure 2.
 The heat kernel graphs for different t .

Furthermore, it follows that (i) $\Phi(x - y, t)$ satisfies the heat equation (**Property 1: translation invariance**) and (ii) $(\Phi * \phi)(x, t) = \int_{-\infty}^{\infty} \Phi(x - y, t) \phi(y) dy$ satisfies the heat equation (**Property 3: integrals and convolutions**).

From the definition ($\Phi = u_x$), by differentiating Eq. (7) with respect to x , we see that $\Phi(x, t)$ satisfies

$$\begin{cases} \Phi_t = D\Phi_{xx} \\ \Phi(x, 0) = u_x(x, 0) = \frac{d}{dx}H(x) \end{cases} \quad (17)$$

Even though $H(x)$ is not differentiable due to discontinuity at $x = 0$, we can redefine differentiation in a broad sense (weak derivative) and under this weak derivative definition:

$$\frac{d}{dx}H(x) = \delta(x) = \begin{cases} 0 & \text{if } x \neq 0 \\ \infty & \text{if } x = 0 \end{cases} \quad (18)$$

where $\delta(x)$ is called the Dirac delta function. The Dirac delta function satisfies a few important properties:

1. $\lim_{t \rightarrow 0^+} \Phi(x, t) = \delta(x)$
2. $\int_{-\infty}^{\infty} \delta(x) dx = 1$ and $\int_{-\infty}^{\infty} \delta(x - y) dx = 1$
3. $\int_{-\infty}^{\infty} \delta(x) f(x) dx = f(0)$ and $\int_{-\infty}^{\infty} \delta(x - y) f(x) dx = f(y)$

The third integration property is sometimes called the *sifting property* of the Dirac delta function. With these properties, we now can show (heuristically) $u(x, t) = (\Phi * \phi)(x, t)$ satisfies the following diffusion equation:

$$\begin{cases} u_t = Du_{xx} \\ u(x, 0) = \phi(x) \end{cases} \quad (19)$$

$$\Rightarrow u(x, t) = (\Phi * \phi)(x, t)$$

To show $(\Phi * \phi)(x, t)$ satisfies the initial condition, we apply the sifting property of the Dirac delta function:

$$\begin{aligned} u(x, 0) &= (\Phi * \phi)(x, 0) \\ &= \int_{-\infty}^{\infty} \Phi(x - y, 0) \phi(y) dy \\ &= \int_{-\infty}^{\infty} \delta(x - y) \phi(y) dy \\ &= \phi(x) \end{aligned} \quad (20)$$

In other words, this result (Eq. (19)) indicates that for any initial value problem, the solution can easily be found as a convolution of the heat kernel and initial data.

2.2 Diffusion equation from the stochastic point of view

In many biological systems, passive transports are often described by Brownian motion or diffusion that is observed in random drifting of pollen grains suspended in a fluid. Suppose a Brownian particle located at the position $x = 0$ when time $t = 0$ has moved randomly on a straight line during time Δt . Since the movement of a Brownian particle is random, the location of the Brownian particle at $t = \Delta t$ will be probabilistic. Especially, for smaller Δt elapsed, the Brownian particle will have a higher chance to be found near the starting location $x = 0$ similar to a normal (or Gaussian) probability distribution with zero mean and a small standard deviation. For this reason, the Brownian motion is often described mathematically by random variables in time, which is called a stochastic process (time-dependent random variable).

If we let X_t be a stochastic process in \mathbb{R}^1 describing the position of a fluorescence molecule at time t , i.e., “ $X_t = x$ ” means that the location of a fluorescence molecule at time t is x , then the probability of the Brownian particle located within the interval $(0, \Delta x)$ at time t will be dependent on both Δx and the previous location:

$$\mathbb{P}\{X_t \in (0, \Delta x) | X_0 = 0\} \quad (21)$$

assuming the initial location is the origin ($X_0 = 0$). Bachelier [14] explicitly calculated this probability as

$$\mathbb{P}\{X_t \in (0, \Delta x) | X_0 = 0\} = \int_0^{\Delta x} \frac{1}{\sqrt{4\pi Dt}} \exp\left(-\frac{x^2}{4Dt}\right) dx \quad (22)$$

where D ($\mu\text{m}^2/\text{s}$) is a diffusion coefficient. The probability density function (the integrand) is the fundamental solution of heat equation (Eq. (14)) that is the normal distribution with standard deviation $\sigma = \sqrt{2Dt}$. Later, Einstein [12] showed that the probability density function of randomly moving particles (Brownian motion) satisfies the diffusion equation with a solution $\Phi(x, t)$ (Eq. (17)).

If $g(y)$ is the probability of a Brownian particle to be found at location y when $t = 0$, i.e., $\mathbb{P}\{X_0 = y\} = g(y)$, then the distribution of the Brownian particles can be determined by solving an initial value problem:

$$\begin{cases} \frac{\partial u}{\partial t} = D \frac{\partial^2 u}{\partial x^2}, \\ u(x, 0) = g(x) \end{cases} \quad (23)$$

which has the solution

$$(\Phi * g)(x) = \int_{-\infty}^{\infty} \frac{1}{\sqrt{4\pi Dt}} \exp\left(-\frac{(x-y)^2}{4Dt}\right) g(y) dy. \quad (24)$$

as in Eq. (19).

2.3 Mean squared displacement

The spreading rate of diffusing particles is quantified by a diffusion coefficient, D , which characterizes a linear relationship between mean squared displacement ($\langle x^2 \rangle$) of a Brownian particle and time, where MSD is defined as

$$\begin{aligned} \langle x^2 \rangle &= \int_{-\infty}^{\infty} x^2 \mathbb{P}\{X_t \in (0, \Delta x) | X_0 = 0\} dx \\ &= \int_{-\infty}^{\infty} x^2 \Phi(x, t) dx. \end{aligned} \quad (25)$$

For a diffusion process, MSD increases linearly in time with the rate of the diffusion coefficient:

$$\langle x^2 \rangle = 2nDt. \quad (26)$$

where n is the spatial dimension (\mathbb{R}^n) for a diffusion process. To derive this relation in 1D (\mathbb{R}), we consider $\frac{\partial}{\partial t} \langle x^2 \rangle$

$$\begin{aligned} \frac{\partial}{\partial t} \langle x^2 \rangle &= \frac{\partial}{\partial t} \int_{-\infty}^{\infty} x^2 \Phi(x, t) dx \\ &= \int_{-\infty}^{\infty} x^2 \frac{\partial}{\partial t} \Phi(x, t) dx \\ &= D \int_{-\infty}^{\infty} x^2 \frac{\partial^2}{\partial x^2} \Phi(x, t) dx \end{aligned} \quad (27)$$

where we used Eq. (17). Notice that by the product rule

$$D \int_{-\infty}^{\infty} \frac{\partial}{\partial x} \left(x^2 \frac{\partial}{\partial x} \Phi(x, t) \right) dx = D \int_{-\infty}^{\infty} 2x \frac{\partial}{\partial x} \Phi(x, t) dx + D \int_{-\infty}^{\infty} x^2 \frac{\partial^2}{\partial x^2} \Phi(x, t) dx \quad (28)$$

By solving for $D \int_{-\infty}^{\infty} x^2 \frac{\partial^2}{\partial x^2} \Phi(x, t) dx$

$$\begin{aligned} D \int_{-\infty}^{\infty} x^2 \frac{\partial^2}{\partial x^2} \Phi(x, t) dx &= D \int_{-\infty}^{\infty} \frac{\partial}{\partial x} \left(x^2 \frac{\partial}{\partial x} \Phi(x, t) \right) dx - \int_{-\infty}^{\infty} 2x \frac{\partial}{\partial x} \Phi(x, t) dx \\ &= D \left[x^2 \frac{\partial}{\partial x} \Phi(x, t) \right]_{-\infty}^{\infty} - D \int_{-\infty}^{\infty} 2x \frac{\partial}{\partial x} \Phi(x, t) dx \\ &= 0 - D \int_{-\infty}^{\infty} 2x \frac{\partial}{\partial x} \Phi(x, t) dx \end{aligned} \quad (29)$$

Next, by integration by parts

$$\begin{aligned} -D \int_{-\infty}^{\infty} 2x \frac{\partial}{\partial x} \Phi(x, t) dx &= -D [2x \Phi(x, t)]_{-\infty}^{\infty} + D \int_{-\infty}^{\infty} 2 \Phi(x, t) dx \\ &= -0 + 2D \end{aligned} \quad (30)$$

Finally, by putting all together

$$\begin{aligned} \frac{\partial}{\partial t} \langle x^2 \rangle &= 2D \\ \langle x^2 \rangle &= 2Dt, \end{aligned} \quad (31)$$

for \mathbb{R}^1 .

3. Fluorescence recovery after photobleaching

3.1 Principles of FRAP

Fluorescence recovery after photobleaching is a fluorescence-based biophysical tool developed in the 1970s to investigate the diffusion process in membranes of live cells. Discovery of the green fluorescent protein (GFP) and the invention of commercial confocal laser scanning microscopes (CLSMs) have broadened the accessibility of FRAP for many researchers in the field, and the applications of FRAP have become widely extended to the study of intracellular protein dynamics [15–18]. Over the four decades, there have been considerable advances in microscope technology. However, the basic principle of FRAP remains the same. In FRAP, fluorescently tagged molecules in a small region of interest (ROI) are irreversibly photobleached using a high-intensity laser source for a short period of time, and

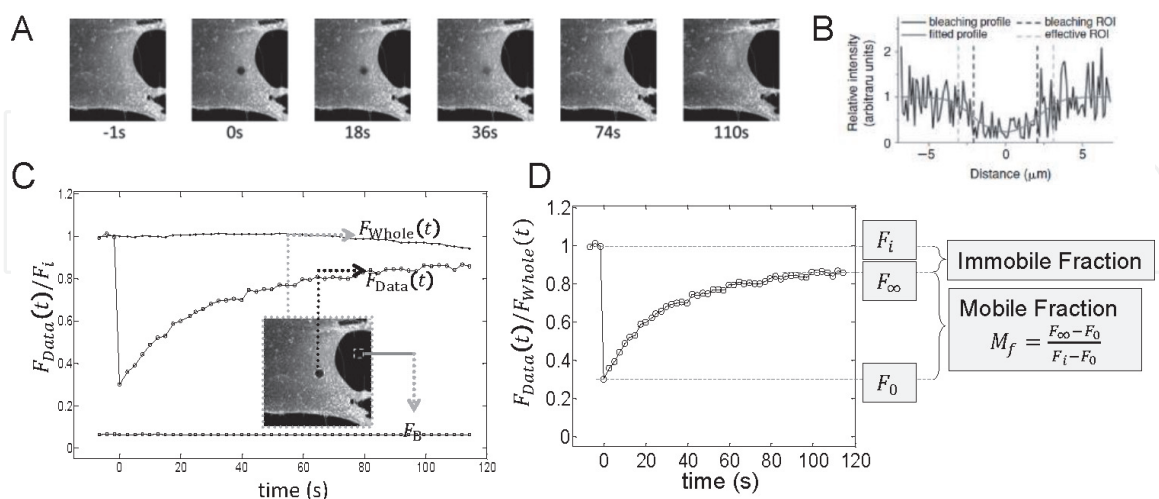


Figure 3. Example of FRAP data. (A) Representative images from a FRAP experiment on Alexa488-CTxB. (B) A postbleach profile from the image for $t = 0$ shows a wider spreading radius (effective radius; r_e) than the bleaching spot radius (nominal radius; r_n) due to diffusion during photobleaching. (C) Mean fluorescence intensity ($N = 13$) from the bleaching ROI (\circ , $F_{Data}(t)$), whole image (\square , $F_{Whole}(t)$), and background (\triangle) from a FRAP experiment of Alexa488-CTxB. The image in the inset shows the locations where $F_{Data}(t)$ (\circ) and background (\square) were measured. (D) In FRAP analysis, prebleach steady-state, postbleach initial, and postbleach steady-state fluorescence intensities are typically denoted as F_i , F_0 , and F_{∞} . These parameters can be used to calculate the mobile fraction (M_f) and the immobile fraction ($1 - M_f$) from the corrected FRAP data for photofading ($F_{Data}(t)/F_{Whole}(t)$) as indicated in the boxed equation.

then the exchange of fluorescence and photobleached molecules in and out of the bleached region is monitored using low-intensity laser excitation to track fluorescence recovery (**Figure 3A**). Due to the artifacts such as the diffusion during the photobleaching step (**Figure 3B**) and the photofading during the imaging step, FRAP data requires some corrections (**Figure 3C**). The diffusion during the photobleaching step can be corrected by using the experimentally measured postbleach profile as an initial condition for the FRAP model [19–21]. On the other hand, the photofading during the imaging step can be corrected by dividing the raw FRAP data ($F_{Data}(t)$) by the fluorescence intensity from the whole image ($F_{Data}(t)$) (**Figure 3D**) [19–21]. Since different transport and reaction mechanisms may affect the curvature and the mobile fraction of a FRAP curve in various manners, kinetic parameters for underlying mechanisms can be obtained by comparing the FRAP curve to the corresponding theoretical FRAP models. For example, D can be measured by comparing a diffusion FRAP model with FRAP data for the best fitting D [19, 20].

3.2 Derivation of diffusion FRAP equation in \mathbb{R}^1

Quantitative FRAP analysis requires a mathematical description of fluorescence recovery for a given underlying transport/reaction kinetics through two different modes of CLSMs: photobleaching and photo-illumination. Although CLSMs use scanning laser for both photobleaching and photo-illumination, it has been reported for small bleaching spot size (we call this as the nominal radius of the laser); the scanning profile of CLSMs on a confocal plane is well approximated by a Gaussian function:

$$I_{r_n}(x) = \sqrt{\frac{2I_0^2}{\pi r_n^2}} \exp\left(-\frac{2x^2}{r_n^2}\right), \quad (32)$$

where r_n is the nominal radius, i.e., radius of a bleaching ROI (the half-width at e^{-2} laser intensity). I_{r_n} can be regarded as a photobleaching mode of CLSMs with a maximal laser intensity I_0 . A bell-shaped profile of $I_{r_n}(x)$ defines total laser intensity I_0 with $\int_{-\infty}^{\infty} I_{r_n}(x) dx = I_0$ resulting from the error function integral (Eq. (11)). Since the high-intensity mode of laser ($I_{r_n}(x)$) causes photobleaching of fluorophores, for illumination, laser intensity has to be attenuated to a lower laser intensity level. Therefore, for an attenuation factor $\epsilon \ll 1$, a photo-illumination mode of CLSMs can be described as $\epsilon I_{r_n}(x)$. If we let $u(x, t)$ be the density of fluorophores (or fluorescent proteins) at a location x at time t , then fluorescence intensity at the position x at time t will be proportional to both the illumination laser intensity ($\epsilon I_{r_n}(x)$) and fluorophore density ($u(x, t)$). Assuming the linear proportionality, $f(x, t)$, the fluorescence intensity at a location (x, y) at time t can be described as

$$f(x, t) = q \cdot \epsilon I_{r_n}(x) u(x, t), \quad (33)$$

where the proportionality constant, q , is referred to as a quantum yield or quantum efficiency. When a CLSM system is used to photobleach fluorophores, its postbleach profile is not exactly the same as the laser profile in most cases due to diffusion occurring during the photobleaching step. Assuming the first-order photobleaching process with a photobleaching rate α , a governing equation for a photobleaching process of freely diffusing fluorescent proteins can be described as a reaction–diffusion equation:

$$\begin{cases} u_t = D\Delta u - \alpha I_{r_n}(x)u \\ u(x, 0) = u_0 \end{cases} \quad (34)$$

where u_0 is the prebleach steady-state fluorescence intensity, which is regarded as a constant. Although the solution to Eq. (34) is hard to find, it is empirically proven [22] that a confocal postbleach profile can be described as a simple Gaussian function (constant minus Gaussian):

$$\varphi(x) = C_i \left(1 - K \exp \left(-\frac{2x^2}{r_e^2} \right) \right), \quad (35)$$

Note that different underlying kinetics for u yield a different FRAP equation. For free diffusion kinetics, the evolution of $u(x, t)$ can be described as the diffusion equation subject to the initial condition from a postbleach profile right after photobleaching.

$$\begin{cases} u_t = D\Delta u \\ u(x, 0) = \varphi(x) \end{cases} \quad (36)$$

where $D(\mu\text{m}^2/\text{s})$ is a diffusion coefficient and the Laplacian, $\Delta = \frac{\partial^2}{\partial x^2}$, in \mathbb{R}^1 . The solution of the diffusion equation can be found as (Eq. (19))

$$\begin{aligned} u(x, t) &= \Phi_D * \varphi \\ &= \int \Phi_D(x - \bar{x}, t) \varphi(\bar{x}) d\bar{x} \\ &= \frac{C_i}{\sqrt{4\pi Dt}} \int \exp \left(-\frac{(x - \bar{x})^2}{4Dt} \right) \left[1 - K \exp \left(-\frac{2\bar{x}^2}{r_e^2} \right) \right] d\bar{x} \\ &= \frac{C_i}{\sqrt{4\pi Dt}} \int \exp \left(-\frac{(x - \bar{x})^2}{4Dt} \right) d\bar{x} - \frac{C_i K}{\sqrt{4\pi Dt}} \int \exp \left(-\frac{(x - \bar{x})^2}{4Dt} - \frac{2\bar{x}^2}{r_e^2} \right) d\bar{x} \quad (37) \\ &= C_i - \frac{C_i K}{\sqrt{4\pi Dt}} \int \exp \left(-\frac{(x - \bar{x})^2}{4Dt} - \frac{2\bar{x}^2}{r_e^2} \right) d\bar{x} \end{aligned}$$

by Eq. (11) (error function integration).

The total fluorescence intensity from the region of interest can be found by integrating this local fluorescence intensity over the ROI:

$$F(t) = q\epsilon \int I_{r_n}(x) u(x, t) dx, \quad (38)$$

which is called a FRAP equation. To simplify Eq. (38) by using Eq. (37)

$$\begin{aligned} &q\epsilon \int I_{r_n}(x) u(x, t) dx \\ &= q\epsilon \int \left[\sqrt{\frac{2I_0^2}{\pi r_n^2}} \exp \left(-\frac{2x^2}{r_n^2} \right) \right] \left[C_i - \frac{C_i K}{\sqrt{4\pi Dt}} \int \exp \left(-\frac{(x - \bar{x})^2}{4Dt} - \frac{2\bar{x}^2}{r_e^2} \right) d\bar{x} \right] dx \end{aligned}$$

$$\begin{aligned}
 &= q\epsilon C_i \sqrt{\frac{2I_0^2}{\pi r_n^2}} \int \exp\left(-\frac{2x^2}{r_n^2}\right) dx - q\epsilon C_i K \sqrt{\frac{2I_0^2}{4\pi^2 r_n^2 Dt}} \iint \exp\left(-\frac{2x^2}{r_n^2} - \frac{(x - \bar{x})^2}{4Dt} - \frac{2\bar{x}^2}{r_e^2}\right) dx d\bar{x} \\
 &= q\epsilon C_i I_0 - q\epsilon C_i K \sqrt{\frac{2I_0^2}{4\pi^2 r_n^2 Dt}} \iint \exp\left(-\frac{2x^2}{r_n^2} - \frac{(x - \bar{x})^2}{4Dt} - \frac{2\bar{x}^2}{r_e^2}\right) dx d\bar{x} \\
 &= F_i - F_i K \sqrt{\frac{1}{2\pi^2 r_n^2 Dt}} \iint \exp\left(-\frac{2x^2}{r_n^2} - \frac{(x - \bar{x})^2}{4Dt} - \frac{2\bar{x}^2}{r_e^2}\right) dx d\bar{x} \quad (39)
 \end{aligned}$$

where $F_i = q\epsilon C_i I_0$ is the prebleach fluorescence intensity due to fluorophore density C_i . If we let $\bar{x} = x + \theta\chi$ where $\theta = \sqrt{4Dt}$ ($d\bar{x} = \theta d\chi$), then the integral term in Eq. (39) becomes

$$\begin{aligned}
 &\iint \exp\left(-\frac{2x^2}{r_n^2} - \frac{(x - \bar{x})^2}{4Dt} - \frac{2\bar{x}^2}{r_e^2}\right) dx d\bar{x} \\
 &= \theta \iint \exp\left(-\frac{2x^2}{r_n^2} - \frac{\theta^2}{\theta^2} \chi^2 - \frac{2(x + \theta\chi)^2}{r_e^2}\right) dx d\chi \\
 &= \theta \iint \exp\left(-\frac{2(r_e^2 x^2 + r_n^2 (x + \theta\chi)^2)}{r_n^2 r_e^2} - \chi^2\right) dx d\chi \\
 &= \theta \iint \exp\left(-\frac{2([r_e^2 + r_n^2]x^2 + 2r_n^2 \theta x\chi + \theta^2 r_n^2 \chi^2)}{r_n^2 r_e^2} - \chi^2\right) dx d\chi \quad (40) \\
 &= \theta \iint \exp\left(-\frac{2[r_e^2 + r_n^2] \left(x^2 + 2\frac{r_n^2 \theta}{r_e^2 + r_n^2} x\chi + \frac{\theta^2 r_n^2}{r_e^2 + r_n^2} \chi^2\right)}{r_n^2 r_e^2} - \chi^2\right) dx d\chi \\
 &= \theta \iint \exp\left(-\frac{2[r_e^2 + r_n^2]}{r_n^2 r_e^2} \left\{ \left(x + \frac{r_n^2 \theta}{r_e^2 + r_n^2} \chi\right)^2 - \left(\left[\frac{r_n^2 \theta}{r_e^2 + r_n^2}\right]^2 - \frac{\theta^2 r_n^2}{r_e^2 + r_n^2}\right) \chi^2 \right\} - \chi^2\right) dx d\chi \\
 &= \theta \iint \exp\left(-\frac{2[r_e^2 + r_n^2]}{r_n^2 r_e^2} \left\{ \left(x + \frac{r_n^2 \theta}{r_e^2 + r_n^2} \chi\right)^2 - \left(\frac{r_n^4 \theta^2 - \theta^2 r_n^4 - \theta^2 r_n^2 r_e^2}{[r_e^2 + r_n^2]^2}\right) \chi^2 \right\} - \chi^2\right) dx d\chi \\
 &= \theta \iint \exp\left(-\frac{2[r_e^2 + r_n^2]}{r_n^2 r_e^2} \left\{ \left(x + \frac{r_n^2 \theta}{r_e^2 + r_n^2} \chi\right)^2 - \left(\frac{-\theta^2 r_n^2 r_e^2}{[r_e^2 + r_n^2]^2}\right) \chi^2 \right\} - \chi^2\right) dx d\chi \\
 &= \theta \iint \exp\left(-\left\{ \frac{2[r_e^2 + r_n^2] \left(x + \frac{r_n^2 \theta}{r_e^2 + r_n^2} \chi\right)^2}{r_n^2 r_e^2} + \frac{2\theta^2}{r_e^2 + r_n^2} \chi^2 \right\} - \chi^2\right) dx d\chi \\
 &= \theta \int \left[\int \exp\left(\frac{2[r_e^2 + r_n^2] \left(x + \frac{r_n^2 \theta}{r_e^2 + r_n^2} \chi\right)^2}{r_n^2 r_e^2}\right) dx \right] \exp\left(-\left[\frac{2\theta^2}{r_e^2 + r_n^2} + 1\right] \chi^2\right) d\chi \\
 &= \theta \int \left[\int \exp\left(\frac{2[r_e^2 + r_n^2]}{r_n^2 r_e^2} x^2\right) dx \right] \exp\left(-\left[\frac{2\theta^2}{r_e^2 + r_n^2} + 1\right] \chi^2\right) d\chi \\
 &= \theta \int \left[\sqrt{\frac{\pi r_n^2 r_e^2}{2(r_e^2 + r_n^2)}} \right] \exp\left(-\left[\frac{2\theta^2}{r_e^2 + r_n^2} + 1\right] \chi^2\right) d\chi
 \end{aligned}$$

$$\begin{aligned}
 &= \theta \sqrt{\frac{\pi r_n^2 r_e^2}{2(r_e^2 + r_n^2)}} \int \exp\left(-\left[\frac{2\theta^2 + r_e^2 + r_n^2}{r_e^2 + r_n^2}\right] \chi^2\right) d\chi \\
 &= \theta \sqrt{\frac{\pi r_n^2 r_e^2}{2(r_e^2 + r_n^2)}} \sqrt{\frac{\pi(r_e^2 + r_n^2)}{2\theta^2 + r_e^2 + r_n^2}} \\
 &= \sqrt{\frac{\pi^2 r_n^2 r_e^2 (4Dt)}{2(8Dt + r_e^2 + r_n^2)}}
 \end{aligned}$$

Therefore

$$\begin{aligned}
 F(t) &= F_i - F_i K \sqrt{\frac{1}{2\pi^2 r_n^2 Dt}} \sqrt{\frac{\pi^2 r_n^2 r_e^2 (4Dt)}{2(8Dt + r_e^2 + r_n^2)}} \\
 &= F_i - F_i K \sqrt{\frac{r_e^2}{8Dt + r_e^2 + r_n^2}} \\
 &= F_i \left[1 - \frac{K}{\sqrt{1 + \gamma^2 + 2t/\tau_D}} \right]
 \end{aligned} \tag{41}$$

where $\gamma = r_n/r_e$ and $\tau_D = r_e^2/(4D)$. If we consider the immobile fraction (**Figure 3D**), the FRAP equation for mobile fluorophores is found as

$$F(t) = F_i \left\{ 1 - \frac{K}{\sqrt{1 + \gamma^2 + 2t/\tau_D}} \right\} \mathbb{M} + (1 - \mathbb{M})F_0 \tag{42}$$

for the mobile fraction, \mathbb{M} is defined as (**Figure 3D**)

$$\mathbb{M} = \frac{F_\infty - F_0}{F_i - F_0} \tag{43}$$

where F_i , F_0 , and F_∞ are prebleach steady-state fluorescence intensity, postbleach initial fluorescence intensity ($F(0)$), and postbleach steady-state fluorescence intensity, respectively. The calculations for the 1D FRAP model can easily be extended to higher-dimensional cases. For example, a diffusion FRAP equation in 2D (\mathbb{R}^2) and 3D (\mathbb{R}^3) is found as

$$\begin{aligned}
 F(t) &= F_i \left[1 - \frac{K}{1 + \gamma^2 + 2t/\tau_D} \right] \text{ (2D)} \\
 F(t) &= F_i \left[1 - \frac{K}{(1 + \gamma^2 + 2t/\tau_D) \sqrt{1 + \gamma^2 + 2t/\tau_D}} \right] \text{ (3D)}
 \end{aligned} \tag{44}$$

4. Fluorescence correlation spectroscopy

4.1 Principles of fluorescence correlation spectroscopy

Fluorescence correlation spectroscopy is a standard bioengineering and biophysics technique for the study of molecular movements and interactions [23–25]. For FCS experiments, a laser beam is focused and stationed at a region of interest in

the specimen (usually live cells). The illumination region formed by the focused laser is called a confocal volume, which is generally in the femtoliter range. As fluorescence molecules cross the confocal volume by diffusion or other transporting mechanisms, they emit fluorescence photons responding to the illumination laser (**Figure 4A**), and the fluctuations in the fluorescence signal, $F(t)$, is monitored as a function of time which is called raw FCS data. Since different FCS measurements from different cells can be quite different depending on the fluorescent protein expression level, the raw FCS data is first standardized by

$$\frac{\Delta F(t)}{\langle F \rangle_t} = \frac{(F(t) - \langle F(t) \rangle_t)}{\langle F \rangle_t} \tag{45}$$

where $F(t)$ is the fluorescence fluctuation in the confocal volume and $\langle F \rangle_t = \frac{1}{T} \int_0^T F(t) dt$ is the time average of the fluorescence fluctuation during observation time T . Notice that the mean of standardized data ($\Delta F(t)/\langle F \rangle_t$) is zero. Next, the autocorrelation function of the standardized data is calculated by multiplying the standardized data, $\Delta F(t)/\langle F \rangle_t$, and the shifted standardized data by τ , $\Delta F(t + \tau)/\langle F \rangle_t$, and then taking the average over time:

$$G(\tau) = \left\langle \frac{\Delta F(t)}{\langle F \rangle_t} \cdot \frac{\Delta F(t + \tau)}{\langle F \rangle_t} \right\rangle_t \tag{46}$$

Notice that the autocorrelation has the maximum when $\tau = 0$ and converges to 0 as τ increases as $\Delta F(t)/\langle F \rangle_t$ and $\Delta F(t + \tau)/\langle F \rangle_t$ become independent for a large τ .

$$\begin{cases} G(0) = \left\langle \left(\frac{\Delta F(t)}{\langle F \rangle_t} \right)^2 \right\rangle_t > 0 \\ G(\tau) = \left\langle \frac{\Delta F(t)}{\langle F \rangle_t} \cdot \frac{\Delta F(t + \tau)}{\langle F \rangle_t} \right\rangle_t = \left\langle \frac{\Delta F(t)}{\langle F \rangle_t} \right\rangle_t \left\langle \frac{\Delta F(t + \tau)}{\langle F \rangle_t} \right\rangle_t = 0 \text{ for a large } \tau \end{cases} \tag{47}$$

An autocorrelation curve carries two crucial information. Since a large molecule will move slower than a light molecule, therefore the correlation decays at a longer time scale. On the other hand, the correlation amplitude is inversely proportional to

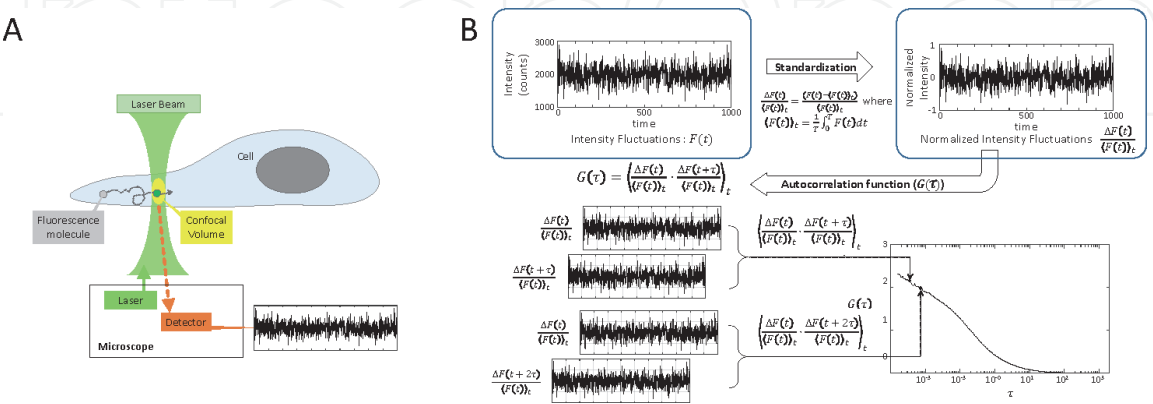


Figure 4. Principles of fluorescence correlation spectroscopy analysis. (A) For FCS analysis for free diffusion, a static laser beam is focused on a specific region of interest. As the fluorescence molecules diffuse in and out of a certain domain, commonly called confocal volume (~1 femtoliter), fluorescence intensities from the confocal volume fluctuate, yielding fluorescence time series. (B) The fluorescence time series data are processed into an autocorrelation curve by taking the average of the original time series data and the shifted time series data by τ to get an autocorrelation function (ACF) in τ . The ACF from the FCS data is next fitted to theoretical autocorrelation functions (ACFs) to determine underlying kinetic parameters, such as a diffusion coefficient.

the concentration of fluorophores due to the denominator for standardization. The information on the diffusion coefficient and concentration of fluorophores can be determined, once a mathematical model for $G(\tau)$ is developed.

Stationarity and ergodicity of the diffusion process play a pivotal role to derive an FCS equation in a closed, yet simple, form. A continuous-time dynamical system such as Brownian motion is called ergodic when all the accessible microstates such as the locations of a Brownian particle are equally probable over a long period, i.e., the statistical properties from the time average at a position are same as the ensemble (spatial) average at any moment. On the other hand, a stationary process is a stochastic process whose probability distribution and parameters are invariant by shifts in time. Stationary and ergodic properties of a diffusion process were proven mathematically [26].

If we let $n(x, t)$ be the fluorescence molecule density per unit area, the temporal average of $n(x, t)$ at a location x_0 and the spatial (ensemble) average of $n(x, t)$ can be defined as

$$\begin{cases} \langle n(x_0, t) \rangle_t = \lim_{T \rightarrow \infty} \frac{1}{T} \int_0^T n(x_0, t) dt \\ \langle n(x, t_0) \rangle = \mathbb{E}(n(x, t_0)) = \int_{-\infty}^{\infty} n(x, t_0) \mathbb{P}\{X_{t_0} = x\} dx. \end{cases} \quad (48)$$

Under stationarity and ergodicity of a diffusion process, we assume

$$\begin{aligned} \langle n(x_0, t) \rangle_t &= \lim_{T \rightarrow \infty} \frac{1}{T} \int_0^T n(x_0, t) dt \\ &= \int_{-\infty}^{\infty} n(x, t_0) \mathbb{P}\{X_{t_0} = x\} dx \quad (\text{Ergodicity}) \\ &= \int_{-\infty}^{\infty} n(x, 0) \mathbb{P}\{X_0 = x\} dx \quad (\text{Stationarity}) \\ &= \langle n(x, 0) \rangle_x \end{aligned} \quad (49)$$

where $n(x, t_0)$ can be thought as a snapshot of all the positions of Brownian particles at any fixed time t_0 .

4.2 Derivation of diffusion FCS equation

For the fluorescence molecule density per unit area, $n(x, t)$, if we let $f(x, t)$ be the fluorescence intensities due to photons from fluorescent proteins at the location x at the time t , then $f(x, t)$ is proportional to $n(x, t)$. On the other hand, since more fluorescence photons can be generated under the higher laser intensity, $f(x, t)$ is also proportional to the laser intensity, $I(x)$. Therefore, $f(x, t)$ satisfies

$$f(x, t) = QI(x)n(x, t) \quad (50)$$

where Q is a proportionality constant for the product of the absorption cross section by the fluorescence quantum yield and the efficiency of fluorescence, and $I(x)$ is a function describing a Gaussian laser profile:

$$I(x) = \sqrt{\frac{2}{\pi\omega^2}} \exp\left(-2\frac{x^2}{\omega^2}\right) \quad (51)$$

where ω is the half-width of the beam at e^{-2} , which measures the size of a confocal volume (V).

A bell-shaped profile of $I(x)$ defines a unit confocal volume (V) with $|V| = \int_{-\infty}^{\infty} I(x)dx = 1$, resulting from the error function integral (Eq. (11)). Therefore, the fluorescent intensity (or the number of photons, $F(t)$) from the confocal volume is determined by

$$\begin{aligned} F(t) &= \int_{-\infty}^{\infty} f(x, t)dx \\ &= Q \int_{-\infty}^{\infty} I(x)n(x, t)dx \\ &= Q \int_V I(x)n(x, t)dx \end{aligned} \quad (52)$$

where we used the fact that the Gaussian laser profile defines the confocal volume in the last equality to switch the integration domain from V to $(-\infty, \infty)$.

Lastly, we will also assume the spatial and temporal independence of fluorescence intensities:

$$\begin{aligned} \langle f(x, t)f(y, t) \rangle_t &= \begin{cases} \langle (f(x, t))^2 \rangle_t & \text{if } x = y \\ \langle f(x, t) \rangle_t \langle f(y, t) \rangle_t & \text{if } x \neq y \end{cases} \\ &= \begin{cases} \langle (f(x, 0))^2 \rangle & \text{if } x = y \\ \langle f(x, 0) \rangle \langle f(y, 0) \rangle & \text{if } x \neq y \end{cases} \end{aligned} \quad (53)$$

This assumption hypothesizes that fluorescence intensities from different locations are not correlated but independent.

In FCS, to analyze the fluorescence fluctuations from the confocal volume (V), an autocorrelation function (ACF) of the variations in $F(t)$ is considered. The variations in the number of photons from the mean number of photons in a confocal volume (ΔF) are calculated by $\Delta F(t) = F(t) - \langle F \rangle_t$ where $F(t)$ and $\langle F \rangle_t$ are the fluorescence intensity in the confocal volume at time t and the mean fluorescence in the confocal volume, respectively. Therefore, by Eq. (52)

$$\begin{aligned} \Delta F(t) &= F(t) - \langle F \rangle_t \\ &= \int_{-\infty}^{\infty} f(x, t)dx - \lim_{T \rightarrow \infty} \frac{1}{T} \int_0^T f(x, t)dt \\ &= Q \int_{-\infty}^{\infty} I(x)n(x, t)dx - \lim_{T \rightarrow \infty} \frac{1}{T} \int_0^T \left[Q \int_{-\infty}^{\infty} I(x)n(x, t)dx \right] dt \\ &= Q \int_{-\infty}^{\infty} I(x)n(x, t)dx - Q \int_{-\infty}^{\infty} I(x)\langle n \rangle_t dx \\ &= Q \int_{-\infty}^{\infty} I(x)\Delta n(x, t)dx \end{aligned} \quad (54)$$

where $\Delta n(x, t) = n(x, t) - \langle n \rangle_t$, we used the identities $\int_{-\infty}^{\infty} I(x)dx = 1$.

Next, the autocorrelation function of the standardized fluorescence fluctuations, $\Delta F / \langle F \rangle_t$, is computed by

$$\begin{aligned}
 G(\tau) &= \left\langle \frac{\Delta F(t)}{\langle F \rangle_t} \frac{\Delta F(t+\tau)}{\langle F \rangle_t} \right\rangle_t \\
 \langle F \rangle_t^2 G(\tau) &= \lim_{T \rightarrow \infty} \int_0^T [\Delta F(t) \Delta F(t+\tau)] dt \\
 &= \langle \Delta F(t) \Delta F(t+\tau) \rangle_t \\
 &= \left\langle \left(Q \int_{-\infty}^{\infty} I(x) \Delta n(x, t) dx \right) \left(Q \int_{-\infty}^{\infty} I(x) \Delta n(x, t+\tau) dx \right) \right\rangle_t \\
 &= Q^2 \int_{-\infty}^{\infty} \int_{-\infty}^{\infty} I(x) I(y) \langle \Delta n(x, t) \Delta n(x, t+\tau) \rangle_t dx dy
 \end{aligned} \tag{55}$$

where we used Eq. (50).

Notice that $n(x, t)$ satisfies the diffusion equation (Eq. (19)).

Therefore, $\Delta n(x, t+\tau)$ also satisfies a diffusion equation in τ and x with initial time at t ($\tau = 0$):

$$\begin{cases} \frac{\partial}{\partial \tau} \Delta n(x, t+\tau) = D \frac{\partial^2}{\partial x^2} \Delta n(x, t+\tau) \\ \Delta n(x, t) = n(x, t) - \langle n \rangle_t \end{cases} \tag{56}$$

Consequently, the solution $\Delta n(x, t+\tau)$ is found as (Eq. (21))

$$\begin{aligned}
 \Delta n(x, t+\tau) &= \int_{-\infty}^{\infty} \Delta n(\bar{x}, t) \frac{1}{\sqrt{4\pi D\tau}} \exp\left(-\frac{(x-\bar{x})^2}{4D\tau}\right) d\bar{x} \\
 &= \int_{-\infty}^{\infty} \Delta n(\bar{x}, t) \Phi(\tau, x-\bar{x}) d\bar{x}.
 \end{aligned} \tag{57}$$

Next, we use the ergodicity of a diffusion process to derive some essential properties of the double integral. Because diffusion is an ergodic process, the time average can be replaced by the ensemble average.

$$\begin{aligned}
 \langle \Delta n(x, t) \Delta n(y, t+\tau) \rangle_t &= \left\langle \Delta n(x, t) \int_{-\infty}^{\infty} \Delta n(\bar{x}, t) \Phi(\tau, y-\bar{x}) d\bar{x} \right\rangle_t \\
 &= \int_{-\infty}^{\infty} \langle \Delta n(x, t) \Delta n(\bar{x}, t) \rangle_t \Phi(\tau, y-\bar{x}) d\bar{x} \\
 &= \int_{-\infty}^{\infty} \langle \Delta n(x, 0) \Delta n(\bar{x}, 0) \rangle \Phi(\tau, y-\bar{x}) d\bar{x} \\
 &= \int_{-\infty}^{\infty} \left\langle (\Delta n(x, 0))^2 \right\rangle \delta(x-\bar{x}) \Phi(\tau, y-\bar{x}) d\bar{x} \\
 &= \sigma^2 \Phi(\tau, y-x)
 \end{aligned} \tag{58}$$

where $\sigma^2 = \langle (\Delta n(x, 0))^2 \rangle$ is the variance of $n(x, 0)$, or the mean square fluctuations of the fluorescence molecules, and $\delta(x-\bar{x})$ is the Dirac delta function defined as Eq. (18). In Eq. (58), the stationary and ergodic assumptions were used in the third line to convert the time average to the spatial average at $t = 0$.

$$\begin{aligned}\langle \Delta n(x, 0) \Delta n(\bar{x}, 0) \rangle &= \begin{cases} \langle (\Delta n(x, 0))^2 \rangle & \text{if } x = \bar{x} \\ \langle \Delta n(x, 0) \rangle \langle \Delta n(\bar{x}, 0) \rangle & \text{if } x \neq \bar{x} \end{cases} \\ &= \begin{cases} \sigma^2 & \text{if } x = \bar{x} \\ 0 & \text{if } x \neq \bar{x} \end{cases} \\ &= \sigma^2 \delta(x - \bar{x})\end{aligned}\quad (59)$$

By plugging Eq. (58) back into Eq. (55)

$$\begin{aligned}\langle F \rangle_t^2 G(\tau) &= Q^2 \int_{-\infty}^{\infty} \int_{-\infty}^{\infty} I(x) I(y) \langle \Delta n(x, t) \Delta n(x, t + \tau) \rangle_t dx dy \\ &= Q^2 \int_{-\infty}^{\infty} \int_{-\infty}^{\infty} I(x) I(y) \sigma^2 \Phi(\tau, y - x) dx dy \\ &= Q^2 \sigma^2 \int_{-\infty}^{\infty} \int_{-\infty}^{\infty} \left[\frac{2}{\pi \omega^2} \exp \left(-\frac{2(x^2 + y^2)}{\omega^2} \right) \right] \left[\frac{1}{\sqrt{4\pi D\tau}} \exp \left(-\frac{(x - y)^2}{4D\tau} \right) \right] dx dy \\ &= Q^2 \sigma^2 \left(\frac{2}{\pi \omega^2} \cdot \frac{1}{\sqrt{4\pi D\tau}} \right) \int_{-\infty}^{\infty} \int_{-\infty}^{\infty} \exp \left(-\frac{2(x^2 + y^2)}{\omega^2} - \frac{(x - y)^2}{4D\tau} \right) dx dy\end{aligned}\quad (60)$$

If we substitute $y = x + \sqrt{4D\tau}\eta$ ($dy = \sqrt{4D\tau}d\eta$), then

$$\begin{aligned}\langle F \rangle_t^2 G(\tau) &= \frac{2Q^2\sigma^2}{\pi\omega^2\sqrt{4\pi D\tau}} \int_{-\infty}^{\infty} \int_{-\infty}^{\infty} \exp \left(-\frac{2(x^2 + (x + \sqrt{4D\tau}\eta)^2)}{\omega^2} - \eta^2 \right) \sqrt{4D\tau} d\eta dx \\ &= \frac{2Q^2\sigma^2}{\pi\sqrt{\pi}\omega^2} \int_{-\infty}^{\infty} \int_{-\infty}^{\infty} \exp \left(-\frac{2(x^2 + (x + \sqrt{4D\tau}\eta)^2) + \omega^2\eta^2}{\omega^2} \right) d\eta dx \\ &= \frac{2Q^2\sigma^2}{\pi\sqrt{\pi}\omega^2} \int_{-\infty}^{\infty} \int_{-\infty}^{\infty} \exp \left(-\frac{2(x^2 + (x + \sqrt{4D\tau}\eta)^2) + \omega^2\eta^2}{\omega^2} \right) d\eta dx\end{aligned}\quad (61)$$

where we used the fact

$$\begin{aligned}&\int_{-\infty}^{\infty} \int_{-\infty}^{\infty} \exp \left(-\frac{2(x^2 + (x + \sqrt{4D\tau}\eta)^2)}{\omega^2} - \eta^2 \right) d\eta dy \\ &= \int_{-\infty}^{\infty} \int_{-\infty}^{\infty} \exp \left(-\frac{4x^2 + 4\sqrt{4D\tau}x\eta + 2(4D\tau)\eta^2 + \omega^2\eta^2}{\omega^2} \right) d\eta dy \\ &= \int_{-\infty}^{\infty} \int_{-\infty}^{\infty} \exp \left(-\frac{4(x^2 + 2\sqrt{D\tau}x\eta + [\sqrt{D\tau}\eta]^2) + [4D\tau + \omega^2]\eta^2}{\omega^2} \right) d\eta dy \\ &= \int_{-\infty}^{\infty} \int_{-\infty}^{\infty} \exp \left(-\frac{4(x + \sqrt{D\tau}\eta)^2 + [4D\tau + \omega^2]\eta^2}{\omega^2} \right) d\eta dy\end{aligned}\quad (62)$$

Now, we can evaluate the inner integral in Eq. (46) using a substitution $z = x + \sqrt{D\tau}\eta$ for x

$$\int_{-\infty}^{\infty} \exp\left(-\frac{4(x + \sqrt{D\tau}\eta)^2}{\omega^2}\right) dx = \int_{-\infty}^{\infty} \exp\left(-\frac{4z^2}{\omega^2}\right) dz \quad (63)$$

$$= \frac{\omega\sqrt{\pi}}{2}$$

where we used Eq. (11). Back to Eq. (61)

$$\begin{aligned} \langle F \rangle_t^2 G(\tau) &= \frac{2Q^2\sigma^2}{\pi\sqrt{\pi}\omega^2} \int_{-\infty}^{\infty} \left\{ \int_{-\infty}^{\infty} \exp\left(-\frac{4(x + \sqrt{D\tau}\eta)^2}{\omega^2}\right) dx \right\} \exp\left(-\frac{(4D\tau + \omega^2)\eta^2}{\omega^2}\right) d\eta \\ &= \frac{Q^2\sigma^2}{\omega\pi} \int_{-\infty}^{\infty} \exp\left(-\frac{(4D\tau + \omega^2)\eta^2}{\omega^2}\right) d\eta \quad (64) \\ &= \frac{Q^2\sigma^2}{\omega\pi} \sqrt{\frac{\omega^2\pi}{4D\tau + \omega^2}} \\ &= \frac{Q^2\sigma^2}{\omega\sqrt{\pi}} \frac{1}{\sqrt{1 + \tau/\tau_D D}} \end{aligned}$$

by the error function integration (Eq. (11)), where $\tau_D = \omega^2/(4D)$, which is a diffusion time.

If fluorescence molecules undergo Brownian motion, then the number of photons in a confocal volume changes in time due to random movements of fluorescence molecules in and out of the confocal volume. In FCS analysis, the number of photons (or fluorescence molecules) from a confocal volume at any moment t is assumed to follow a Poisson distribution, in which the probability for k fluorescence molecules (or photons) to be found in the confocal volume is

$$\mathbb{P}(F(t) = k) = \frac{e^{-\lambda} \lambda^k}{k!} \quad (65)$$

where $\lambda = \langle F \rangle_t$ is the average number of fluorescence molecules (or photons) in the confocal volume. This assumption is reasonable for a diffusion process since the arrival process of infinitely many identical independent diffusion processes was shown to be a Poisson process [27]. Importantly, the mean (or expectation) and variance of a Poisson random variable are known to be equal

$$\begin{cases} \mathbb{E}(F(t)) = \sum_{k=0}^{\infty} k \mathbb{P}\{F(t) = k\} = \langle F \rangle_t \\ \sigma^2 = \mathbb{E}\left(|F(t) - \langle F \rangle_t|^2\right) = \langle F \rangle_t \end{cases} \quad (66)$$

Since we assumed that $F(t)$ follows the Poisson statistics that has equal variance and mean

$$\begin{aligned} \langle F \rangle_t^2 G(0) &= \langle \Delta F(t) \Delta F(t+0) \rangle_t \\ &= \left\langle (\Delta F(t))^2 \right\rangle_t \end{aligned} \quad (67)$$

$$= \sigma^2$$

$$= \langle F \rangle_t$$

by Eq. (66). On the other hand, by Eq. (64)

$$G(0) = \frac{Q^2 \sigma^2}{\omega \sqrt{\pi}} \quad (68)$$

which indicates that

$$\frac{1}{\langle F \rangle_t} = \frac{Q^2 \sigma^2}{\omega \sqrt{\pi}} \quad (69)$$

By replacing the bulk parameters in Eq. (47) with $1/\langle F \rangle_t$

$$G(\tau) = \frac{1}{\langle F \rangle_t} \frac{1}{\sqrt{1 + \tau/\tau_D}} \quad (70)$$

As we saw, with a Poisson distribution assumption on $F(t)$, we can readily determine the average density of fluorescence molecules as well as the average number of fluorescence molecules in the confocal volume. Similar to FRAP equations, FCS equations in higher spatial dimensions can be found by similar calculations

$$G(\tau) = \frac{1}{\langle F \rangle_t} \frac{1}{\left(1 + \tau/\tau_{D_{xy}}\right)} \quad (2D) \quad (71)$$

$$G(\tau) = \frac{1}{\langle F \rangle_t} \frac{1}{\left(1 + \tau/\tau_{D_{xy}}\right) \sqrt{1 + \tau/\tau_{D_z}}} \quad (3D)$$

where $\tau_{D_{xy}} = \omega_{xy}^2/(4D)$ and $\tau_{D_z} = \omega_z^2/(4D)$ with ω_{xy} = the half-width of the beam at e^{-2} in x/y - direction and ω_z = the half-width of the beam at e^{-2} in z - direction.

5. Conclusion

Diffusion plays a crucial role within biological systems in many different temporal and spatial scales from various perspectives. It is a dominant way for biological organisms to transport multiple molecules to desirable locations for cell signaling. However, to quantify the molecular diffusion, especially in live cells, is still challenging although a couple of tools are available, including fluorescence recovery after photobleaching and fluorescence correlation spectroscopy. Although FRAP and FCS were originally developed to study biological diffusion processes, they are now being applied not only to a diffusion process but also to a broad range of biochemical processes, including binding kinetics and anomalous diffusion. Since the derivation of FRAP and FCS equations for many biochemical processes shares many common steps with the diffusion FRAP and FCS equations, it is essential to understand the mathematical theory behind the diffusion FRAP /FCS equation [18, 22, 25, 28–32]. In this study, we provide a simple and straightforward derivation of FRAP/FCS equation for free diffusion based on calculus-level mathematics, so that FRAP/FCS equations and its applications are accessible to a broad audience. Although the applications of these FRAP and FCS equations to cell membrane

biophysics from experimental perspectives can be a very important topic, it is beyond the scope of this chapter and therefore will not be covered here. These topics are well documented in various references, and interested readers are referred to [20, 31, 33], and references therein. We hope that this tutorial is understandable as well as gives readers a solid theoretical foundation for FRAP and FCS, bridging the gap between experimental and theoretical aspects of FRAP and FCS.

IntechOpen


IntechOpen

Author details

Minchul Kang
Department of Mathematics, Texas A&M University-Commerce, Commerce,
TX, USA

*Address all correspondence to: minchul.kang@tamuc.edu

IntechOpen

© 2020 The Author(s). Licensee IntechOpen. Distributed under the terms of the Creative Commons Attribution - NonCommercial 4.0 License (<https://creativecommons.org/licenses/by-nc/4.0/>), which permits use, distribution and reproduction for non-commercial purposes, provided the original is properly cited. 

References

- [1] Murray J. *Mathematical Biology: I. An Introduction (Interdisciplinary Applied Mathematics)*. 3rd ed. New York: Springer; 2007
- [2] Murray J. *Mathematical Biology II: Spatial Models and Biomedical Applications (Interdisciplinary Applied Mathematics)*. 3rd ed. New York: Springer; 2011
- [3] Okubo A, Levin S. *Diffusion and Ecological Problems, Modern Perspectives*. 2nd ed. New York: Springer; 2002
- [4] Ritchie K, Spector J. Single molecule studies of molecular diffusion in cellular membranes: Determining membrane structure. *Biopolymers*. 2007;**87**(2–3): 95-101
- [5] Skaug MJ, Faller R, Longo ML. Correlating anomalous diffusion with lipid bilayer membrane structure using single molecule tracking and atomic force microscopy. *The Journal of Chemical Physics*. 2011;**134**(21):215101
- [6] Das BB, Park SH, Opella SJ. Membrane protein structure from rotational diffusion. *Biochimica et Biophysica Acta*. 2015;**1848**(1 Pt B): 229-245. DOI: 10.1016/j.bbamem.2014.04.002
- [7] Axelrod D, Koppel DE, Schlessinger J, Elson E, Webb WW. Mobility measurement by analysis of fluorescence photobleaching recovery kinetics. *Biophysical Journal*. 1976; **16**(9):1055-1069
- [8] Elson EL, Magde D. Fluorescence correlation spectroscopy. I. Conceptual basis and theory. *Biopolymers*. 1974;**13**: 1-27
- [9] Crank J. *The Mathematics of Diffusion (Oxford Science Publications)*. 2nd ed. USA: Oxford University Press; 1980
- [10] Carslaw HS, Jaeger JC. *Conduction of Heat in Solids (Oxford Science Publications)*. 2nd ed. USA: Oxford University Press; 1986
- [11] Fick A. On liquid diffusion. *Annalen Der Physik und Chemie Ergänzung*. 1885;**94**:59
- [12] Einstein A. Über die von der molekularkinetischen Theorie der Wärme geforderte Bewegung von in ruhenden Flüssigkeiten suspendierten Teilchen. *Annalen der Physik*. 1905; **322**(8):549-560
- [13] von Smoluchowski M. Zur kinetischen theorie der brownschen molekularbewegung und der suspensionen. *Annalen der Physik*. 1906;**326**(14):756-780
- [14] Bachelier L. Théorie de la spéculation. *Annales Scientifiques de l'École Normale Supérieure*. 1900;**17**(3): 21-86
- [15] Carrero G, Crawford E, Hendzel MJ, de Vries G. Characterizing fluorescence recovery curves for nuclear proteins undergoing binding events. *Bulletin of Mathematical Biology*. 2004;**66**: 1515-1545
- [16] Sprague BL, Pego RL, Stavreva DA, McNally JG. Analysis of binding reactions by fluorescence recovery after photobleaching. *Biophysical Journal*. 2004;**86**(6):3473-3495
- [17] Houtsmuller AB. Fluorescence recovery after photobleaching: Application to nuclear proteins. *Advances in Biochemical Engineering/ Biotechnology*. 2005;**95**:177-199
- [18] Kang M, Day CA, DiBenedetto E, Kenworthy AK. A quantitative approach to analyze binding diffusion kinetics by confocal FRAP. *Biophysical Journal*. 2010;**99**(9):2737-2747

- [19] Kang M, Kenworthy A. Complex applications of simple FRAP on membranes. In: Faller R et al., editors. *Biomembrane Frontiers*. New York, USA: Humana Press; 2009
- [20] Day CA, Kraft LJ, Kang M, Kenworthy AK. Analysis of protein and lipid dynamics using confocal fluorescence recovery after photobleaching (FRAP). *Current Protocols in Cytometry*. 2012. Chapter 2; Unit 2.19
- [21] Kang M, Andreani M, Kenworthy AK. Normalizations, scaling, and photo-fading corrections for FRAP data analysis and their implications. *PLoS One*. 2015;**10**(5):e0127966
- [22] Kang M, Day CA, Drake K, Kenworthy AK, DiBenedetto E. A generalization of theory for two-dimensional fluorescence recovery after photobleaching applicable to confocal laser scanning microscopes. *Biophysical Journal*. 2009;**97**(5):1501-1511
- [23] Elson EL. Fluorescence correlation spectroscopy: Past, present, future. *Biophysical Journal*. 2011;**101**(12):2855-2870
- [24] Medina MA, Schwille P. Fluorescence correlation spectroscopy for the detection and study of single molecules in biology. *BioEssays*. 2002;**24**(8):758-764
- [25] Lee K, Astudillo N, Kang M. A simple derivation of diffusion fluorescence correlation spectroscopy equations. *Journal of Fluorescence*. 2020. DOI: 10.1007/s10895-019-02476-z [Epub ahead of print]
- [26] Derman C. Ergodic property of the Brownian motion process. *Proceedings of the National Academy of Sciences of the United States of America*. 1954;**40**(12):1155-1158
- [27] Nadler B, Schuss Z. The stationary arrival process of independent diffusers from a continuum to an absorbing boundary is Poissonian. *SIAM Journal on Applied Mathematics*. 2001;**62**(2):433-447
- [28] Kang M, Kenworthy A. A closed-form analytic expression for FRAP formula for the binding diffusion model. *Biophysical Journal*. 2008;**95**(2):L13-L15
- [29] Kang M, DiBenedetto E, Kenworthy A. Proposed correction to Feder's anomalous diffusion FRAP equations. *Biophysical Journal*. 2011;**100**(3):791-792
- [30] Kang M, Day CA, Drake K, Kenworthy A, DiBenedetto E. Simplified equation to extract diffusion coefficients from confocal FRAP data. *Traffic*. 2012;**13**(12):1589-1600
- [31] Kang M, Andreani M, Kenworthy A. Validation of normalizations, scaling, and photofading corrections for FRAP data analysis. *PLoS One*. 2015;**10**(5):e0127966
- [32] Kang M, Day CA, Drake K, Kenworthy A. A novel computational framework for $D(t)$ from fluorescence recovery after photobleaching data reveals various anomalous diffusion types in live cell membranes. *Traffic*. 2019;**20**(11):867-880
- [33] Chiantia S, Ries J, Schwille P. Fluorescence correlation spectroscopy in membrane structure elucidation. *Biochimica et Biophysica Acta*. 2009;**1788**(1):225-233